

Numerical modelling of a single-compression multi-temperature ejector-supported R744 refrigeration unit for last mile delivery

Modélisation numérique d'un groupe frigorifique au R-744 à compression unique et à température variable assisté par un éjecteur pour la livraison du dernier kilomètre

Francesco Fabris^{a,*}, Jakub Bodys^b, Sergio Marinetti^a, Silvia Minetto^a, Jacek Smółka^b, Antonio Rossetti^a

^a National Research Council, Construction Technologies Institute (CNR-ITC), Padova, 35127, Italy

^b Silesian University of Technology, Institute of Thermal Technology, Konarskiego 22, Gliwice 44-100, Poland

ARTICLE INFO

Keywords:

Refrigeration
Carbon Dioxide
Refrigerated transport
Multi-temperature transport
Ejector

Mots clés:

Froid [artificiel]
Dioxyde de carbone
Transport frigorifique
Transport multi-température
Éjecteur

ABSTRACT

A novel R744 vapor-compression refrigeration system has been developed to meet the cooling needs of a medium-size refrigerated truck at two temperature levels: 4-5 kW for medium-temperature (MT) refrigeration at 0°C and 1-2 kW for low-temperature (LT) refrigeration at -20°C. This system is designed for transporting chilled and frozen goods efficiently during last-mile deliveries in urban areas.

The key innovation of this system lies in its single compression stage with two different evaporation levels. Firstly, the unit incorporates an MT ejector to enhance energy efficiency by reducing the compressor pressure ratio. Furthermore, an LT ejector is employed to allow providing LT cooling with a single-stage compressor by pre-compressing vapor before it enters the compressor, avoiding excessive compression ratios. This extends the LT operational range with a single stage of compression from 34°C to 40°C ambient temperature. When the ambient temperature is not sufficient to sustain the ejector cycle, the system can switch to a back-pressure cycle.

A numerical model of this refrigeration system has been developed to evaluate its steady-state and dynamic performance in both back-pressure and ejector configurations. For a specific cooling effect production (3.8 kW in MT, 1.1 kW in LT operation), the ejector cycle increases the COP by 25.8% for MT and 42.0% for LT operation compared to the back-pressure cycle. However, the back-pressure cycle offers greater flexibility in cooling power production, ranging from -32.8% to +8.2% for MT and -8.9% to +82.5% for LT, making it useful for pulldown and part-load operations.

1. Introduction

Traditionally, temperature-controlled transport and logistics organization were set to distribute separately products characterized by different specific temperature requirements. However, in the last few years the employment of trucks equipped with multiple temperature-specific compartments is becoming more and more common in the market, as such a solution allows to simultaneously transport different product segments (e.g. fresh products at 0°C, frozen products at -20°C and dry products) in separate chambers of the same truck, especially for last mile delivery in urban environment (Frank et al., 2021). As reported in the literature (Ostermeier et al., 2021), significant beneficial effects in

logistics organization can be achieved thanks to multi-temperature transport solutions, such as the reduction of the total duration and mileage of delivery missions, of the number of stops at delivery points and of the total number of vehicles on the road (which is a crucial issue especially in urban areas, due to localized pollution), and significant economic advantages can be achieved as well (Heßler, 2021). A recent study by Fertel et al. (2023) related to the road transport refrigeration fleet in France reports that 26% of the national fleet was equipped with multi-temperature units in 2021, with an increasing trend compared to 2015, in which multi-temperature equipped vehicles were 23% of the national fleet.

Multi-temperature transport refrigeration units currently available in the market employ HFC or HFO refrigerants, such as R452A and

* Corresponding author.

E-mail address: francesco.fabris@itc.cnr.it (F. Fabris).

<https://doi.org/10.1016/j.ijrefrig.2024.01.014>

Received 21 September 2023; Received in revised form 3 January 2024; Accepted 11 January 2024

Available online 12 January 2024

0140-7007/© 2024 The Author(s). Published by Elsevier B.V. This is an open access article under the CC BY license (<http://creativecommons.org/licenses/by/4.0/>).

Nomenclature		Greek letters	
COP	coefficient of performance [-]	ϕ	entrainment ratio [-]
p	pressure [kPa]	<i>Subscripts</i>	
Δp_{lift}	pressure lift [kPa]	amb	ambient
P	power [kW]	comp	compressor
Q	cooling effect [kW]	ev	evaporator
r_p	compressor pressure ratio [-]	HP	high pressure
T	temperature [K]	i	internal
<i>Acronyms</i>		max	maximum
EV	expansion valve	min	minimum
HPV	high-pressure valve	sat	saturation
LT	low temperature	suction	ejector suction nozzle
MT	medium temperature		

R404A. Cavalier et al. (2023) report that, in 2015, 94.6% of new road refrigerated transport equipment in France was employing R404A as the refrigerant, while in 2022 94.5% of new equipment is based on the use of R452A. R404A is almost no more used in new equipment (0.2% in 2022), but old units employing it are still considerably present in the national fleet (81.0% of the total refrigerant mass employed in temperature-controlled transport in 2022). However, sustainability challenges, supported by regulations such as the EU F-Gas Regulation 517/2014 (European Commission, 2014) are exponentially increasing the interest in natural refrigerants (in particular carbon dioxide, R744, and hydrocarbons, HCs) in newly developed transport refrigeration units. A complete review on the employment of natural working fluids in refrigerated transport applications can be found in Minetto et al. (2023).

Being food systems responsible for 20% to almost 40% of total greenhouse gas emissions, the ENOUGH project (<https://enough-emissions.eu/>) supports the EU farm to fork sustainable strategy by providing technical, financial, and political tools and solutions to reduce GHG emissions (by 2030) and achieve carbon neutrality (by 2050) in the food industry. In this context, ENOUGH also addresses transport refrigeration, by proposing solutions which use natural refrigerants (CO₂) and are suitable for integration with renewables (PV), for use of Thermal Energy Storage (TES) and ready for electrification.

Multi-temperature units employing R744 as the refrigerant are developed and available in the market mostly for commercial stationary applications (Gullo et al., 2018; Karampour and Sawalha, 2018; Azzolin et al., 2021). The employment of ejectors for the partial recovery of expansion work to provide a pressure lift to the refrigerant mass flow rate at the evaporators outlet has been proven as a consolidated solution to enhance the R744 transcritical cycle efficiency, whether at medium-temperature level (Pardiñas et al., 2018; Gullo et al., 2019) or low-temperature level (Peris Pérez et al., 2021; Yang et al., 2022). However, in such multi-temperature stationary systems, a subcritical compression stage is always included to increase the refrigerant pressure from the LT evaporation pressure to the suction pressure of the transcritical MT compressors, thus implementing a two-stage compression cycle for the LT operations. Innovative solutions based on the use of ejectors to completely replace the subcritical compression are proposed in a few studies in the literature (Bai et al., 2017; Banasiak et al., 2019), but still considering commercial refrigeration applications, which are characterized by significantly larger cooling demands and larger components dimensions (e.g. ejector dimensions).

Since compactness and weight reduction represent a crucial factor on the overall carbon footprint of a road transport refrigeration unit (Fabris et al., 2023a), the removal of the subcritical compressor from a multi-temperature system schematic would allow a significant reduction in weight, as well as in size and cost, having an ever more significant impact in road transport refrigeration applications than in commercial

refrigeration applications. To this extent, Fabris et al. (2023b) presented a first simplified R744 multi-temperature cooling unit schematic which employed an ejector to replace the subcritical compression stage and provide the necessary pressure lift from the LT evaporation pressure to the MT evaporation pressure and performed an experimental assessment of a commercially available ejector when employed in such operating conditions.

In this study, to avoid operational issues and to comply with the test procedures defined in Annex 1 of the ATP agreement (United Nations, 2022), which requires the operation of MT and LT evaporators independently, an improved version of the preliminary R744 multi-temperature schematic presented in Fabris et al. (2023b) is proposed, in which the employment of two separate ejectors (an MT ejector and a LT ejector) allows the necessary operational flexibility.

The novel cycle architecture proposed in this study, developed for multi-temperature goods road transport for last-mile deliveries, can represent a sustainable and efficient solution for the reduction of the total carbon footprint of road transport refrigeration systems in urban environment, thanks to the employment of a natural refrigerant (R744) and to the implementation of ejectors, specifically designed and developed for this application, to improve the cycle efficiency and to allow operation both at MT and LT levels with a single stage compressor.

In this study, a dynamic numerical model of the cooling unit has been developed, allowing both steady-state and dynamic evaluation of the cooling unit operation. Simulation results help providing an assessment of the proposed cooling unit performance when operating under different conditions (with or without ejectors, with MT or LT cooling effect production) and understanding the system dynamic behaviour during configuration switches.

2. The refrigeration system

The R744 refrigeration unit proposed in this study is designed to fulfil the refrigerating needs of a multi-temperature refrigerated vehicle, employed for last mile delivery of chilled and frozen goods in urban environment. The design cooling power is 4-5 kW of Medium-Temperature (MT) refrigeration at 0°C air temperature and 1-2 kW of Low-Temperature (LT) refrigeration at -20°C air temperature.

The schematic of the cooling unit is presented in Fig. 1. The proposed design allows operations by a simple back-pressure cycle or through the employment of an MT ejector and of an LT ejector for MT or LT operation, respectively. In both MT and LT operations, the same single-stage compressor is used. The schematic in each of these configurations is highlighted in Fig. 2, in which the red colour is used for the high-pressure level in the gas cooler, the green colour for medium-pressure level, for MT refrigeration, and blue refers to low-pressure level, for LT refrigeration. In the ejector cycle schematics, the light green and light

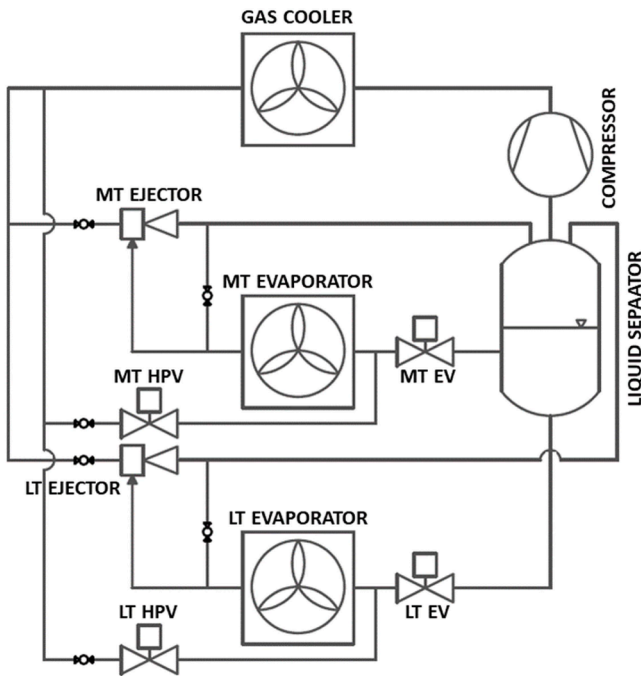


Fig. 1. Simplified schematic of the refrigeration system.

blue colour are used to highlight the pressure lift provided by the dedicated ejector between evaporation and compressor suction.

In the simple back-pressure cycles (Fig. 2(a) and 2(c)), a high-pressure valve (HPV) is used for the expansion of the refrigerant mass flow rate to the evaporation pressure level, while controlling the correct pressure in the gas cooler. The refrigerant evaporates and then reaches the liquid separator as the ejector ports and the EV valves are closed. In this configuration, the compressor speed can be varied through an inverter with frequency between 30 Hz and 70 Hz with effects on the cooling effect production and cycle efficiency, as it will be further discussed in Section 4.1. On the other hand, in the ejector cycles (Fig. 2(b) and 2(d)), the compressor speed is adjusted to control the high-pressure value, while the HPV's are fully closed. The opening of the expansion valve (EV) is adjusted to modify the pressure lift provided by the ejector.

The ejectors reduce the compressor pressure ratio, providing a positive effect on the system Coefficient of Performance (COP), as it will be further discussed in Section 4.2. Despite the use of a single-stage compressor, the pressure lift provided by the ejectors avoids excessive compressor pressure ratio, which could exceed the compressor application limits under harsh environmental temperature conditions, as it will be highlighted in Sections 4.1 and 4.3.

It is worth mentioning that, in case of simultaneous requirement of MT and LT cooling effect, the MT side can be engaged together with the LT side of the system, operating with the separator at a low-pressure level until the LT cooling effect requirement ceases, and the liquid separator pressure can be increased to medium-pressure level again.

2.1. Components dimensioning

Compressor and heat exchangers are chosen among commercially available components. In particular, a R744 semi-hermetic compressor with a displacement volume equal to 16.8 cm^3 is considered. The internal and external convective surfaces of the heat exchangers are equal to 2.1 m^2 and 16.9 m^2 for the gas cooler, 3.8 m^2 and 39.4 m^2 for the MT evaporator and 1.3 m^2 and 8.7 m^2 for the LT evaporator, respectively.

Conversely, the MT and LT ejectors have been specifically designed for this application, as further described in the next section. The ejectors are characterized by a fixed geometry, with a throat diameter at the motive nozzle equal to 0.95 mm for the MT ejector and 0.46 mm for the

LT ejector.

2.2. Ejectors design and performance

Following the experimental results obtained with a commercially available non-optimized ejector (Fabris et al., 2023b), a specific design process of the MT ejector and the LT ejector to be used in this refrigeration system was performed.

Firstly, the capacity of the motive nozzle was selected based on design LT and MT cooling effect of 1.0 kW and 4.5 kW , and corresponding LT and MT evaporator mass flow rate of 0.0072 kg/s and 0.0301 kg/s , respectively. Namely, the diameters of the motive nozzle throats were dimensioned as 0.464 mm and 0.950 mm for LT and MT ejectors, respectively.

Then, the initial dimensioning was proposed basing on the previously developed geometries presented in Palacz et al. (2015). The initial design was optimized using a genetic algorithm involving six characteristic dimensions of motive nozzle and mixing section and two sets of boundary conditions - 86 bar and 35°C for motive nozzle inlet and proper conditions of the LT and MT evaporator outlet for suction nozzle inlet. The design and optimization platform developed in Smolka et al. (2013) and validated in Palacz et al. (2015) was used. The platform incorporated commercial software (Ansys, 2023) and in-house developed code for repeatable mesh generation, iterating solving process and data post-processing. The pressure-based solver was used with the coupled scheme for the pressure-velocity coupling. The spatial discretization scheme called PRESTO! (Ansys, 2023) was used for the pressure, while the other variables were solved with second order upwind scheme. The gradients were evaluated using Green-Gauss Cell Based method. Finally, $k-\epsilon$ turbulence model with enhanced wall treatment was used for turbulence modelling. At the end of the solving process, the levels of the residuals were below a value of 10^{-5} for all the governing equations. Additionally, a mass imbalance was monitored until its level was reduced to below 0.01% of the suction nozzle mass flow rate.

The resulting optimized design provided high-efficiency performance for pressure lift of 4 bar and 5 bar in order to provide the design cooling power at rated operating conditions (ambient temperature of 30°C). Then, a series of 2-D CFD-based numerical simulations were carried out to numerically assess the performance of the ejectors (entrainment ratio, ejector efficiency) under various operating conditions (motive nozzle temperature and pressure, suction nozzle temperature and pressure, pressure lift) and the performance maps of the ejectors were then obtained through interpolation of the numerical results. In total, 128 and 158 operating points utilizing 6 and 9 evaporation levels, 3 motive nozzle inlet conditions and several pressure lift values were simulated for the MT and LT ejectors, respectively. The recorded maximum efficiency (formulated by Elbel and Hrnjak, 2008) was at the level of 36% with corresponding mass entrainment ratio of 0.80 .

As an example, the interpolated performance maps of the MT and LT ejectors for motive nozzle conditions equal to $T_{motive} = 35^\circ\text{C}$ and $p_{motive} = 86 \text{ bar}$ are reported in Fig. 3. The design and optimization approach adopted is in accordance with the one described in previous papers published by the same authors: Smolka et al. (2013), Palacz et al. (2015), Bodys et al. (2017) and Haida et al. (2018).

3. Numerical model of the refrigeration system

A dynamic numerical model of the refrigeration system was developed using the commercial multi-physics software Simcenter Amesim 2021. The numerical approach of the software is based on the discretization of real components in lumped parameters elements, connected to describe the entire system. Each element is described by nonlinear time-dependent differential equations involving the state variables. Equations are assembled in a system of differential equations,

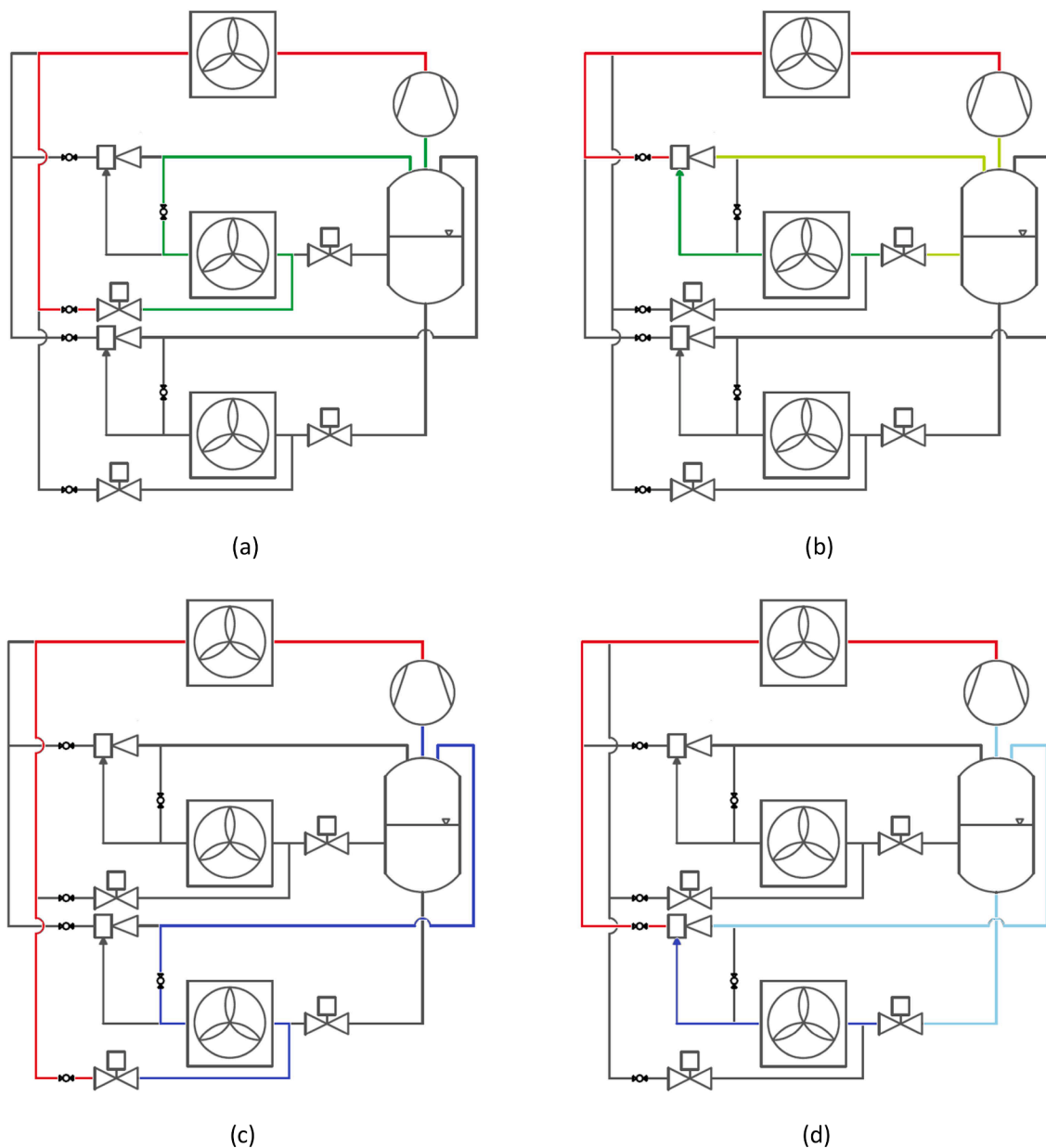


Fig. 2. Operational schematic of the refrigeration system: (a) MT back-pressure cycle; (b) MT ejector cycle; (c) LT back-pressure cycle; (d) LT ejector cycle.

according to the elements connection. The model dynamic is then solved by integrating the system of differential equations over time. This approach allows to solve fast dynamics without the limiting assumptions of the quasi-stationary formulation. The numerical solver adapts the integrating time step at every solving iteration, reducing it to increase the precision in correspondence of highly unsteady operation. A mixed (absolute and relative) residual error estimator is used to check the convergence at each time step: for each state variable y_i , the error must satisfy the conditions $\varepsilon_i < 10^{-7}(1 + y_i)$, thus interpreting the tolerance as an absolute value for small variables ($y_i \ll 1$) and as a relative error for variables with high magnitude ($y_i \gg 1$). The final variable values are saved for post-process with a frequency of 1 Hz.

The numerical model of the cooling unit is developed under the assumptions of homogeneous fluid model for the refrigerant, considering the two phases (liquid and vapor) to flow as a single phase characterized by mean fluid properties and with no slip and thermodynamic equilibrium between the two phases. The internal flow (refrigerant side) is considered one-dimensional, while the external flow (air side) is considered zero-dimensional.

The compressor was modelled using a fixed displacement compressor model. From the compressors operating data available in the commercial data sheets (Dorin, 2022), the different volumetric efficiency and the overall compression efficiency were interpolated as functions of the pressure ratio and the rotational speed. The compressor was assumed to allow operation at variable speed, with frequency between 30 Hz and 70 Hz.

The gas cooler was discretized into $N = 18$ lumped volumes, to better describe the sharp properties changes of the R744 refrigerant in supercritical conditions inside the heat exchanger, while the MT evaporator and the LT evaporator were discretized into $N = 6$ and $N = 4$ lumped volumes, respectively. For all the heat exchangers, each discretized volume was then sub-divided in 3 nodes, one referring to the refrigerant flow, one to the state of tube wall and fins and one referring to the state of the air. The geometric characteristics of the heat exchanger, such as exchange areas and mass, were equally distributed in each lumped element. For the heat exchange between refrigerant and air, internal convection between the refrigerant and the internal wall, conduction through wall and fins and external convection between the fins and the

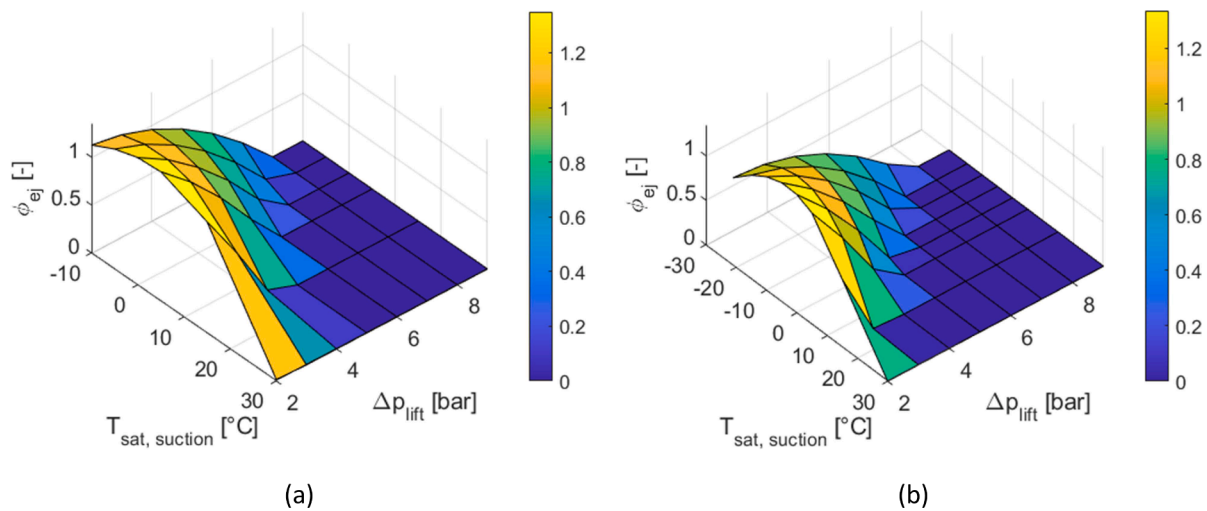


Fig. 3. Interpolated performance maps of the ejectors for $T_{motive} = 35^{\circ}\text{C}$ and $p_{motive} = 86$ bar: (a) MT ejector; (b) LT ejector.

outside air were considered for each of the lumped volumes in which the heat exchangers were discretized. For the refrigerant, mass and energy balances were evaluated in each discretized element in the flow direction. The heat transfer coefficients were evaluated through empirical correlations, available in the literature: for the refrigerant side, Gnielinski correlation for single-phase (Gnielinski, 1976), Shah correlation (Shah, 1979) for two-phase condensation, VDI for horizontal tubes correlation (Steiner and Taborek, 1992) for two-phase boiling; for the air side, Colburn j-factor (McQuiston, 1978).

The liquid separator was modelled as a cylindrical-shape tank with constant cross-sectional area, homogeneous pressure in the entire volume and homogeneous densities for the liquid phase and the vapor phase, in their respective volumes.

The ejectors performance was modelled through implementation of the performance maps obtained from the CFD numerical simulations of the ejectors, as mentioned in Section 2.2, into the physical model of the cooling unit. For each time step, the boundary conditions at the ejector ports (motive nozzle, suction nozzle, discharge port) were used to determine the performance of the ejectors through linear interpolation of the ejector performance maps. The conditions at the ejector ports were then provided as inputs to the lumped parameters volumes describing the rest of the cooling unit, thus allowing to determine the operating conditions of the system at the next time step.

Pressure losses are considered in every pipe element in which the refrigerant circuit is subdivided. In single phase flow conditions, Churchill correlation (Churchill, 1977) is used to compute the regular friction coefficient and evaluate the pressure losses. On the other hand, the pressure drops for the two-phase refrigerant inside the heat exchangers coils are evaluated through Friedel correlation (Friedel, 1979).

The performance of the cooling unit is not affected by the refrigerant charge, if the liquid separator is not emptied or completely filled by liquid refrigerant in all the possible operating conditions. In the numerical simulations described in this study, a refrigerant charge equal to 40 kg of carbon dioxide was found sufficient to guarantee the presence of two-phase mixture in the liquid separator in all the investigated operating conditions. The refrigerant charge is not varied between different simulations or operating conditions. It is worth mentioning that no optimization of the system volume and of the refrigerant charge is performed of this study, as the focus of this paper is the cooling unit performance evaluation. Thus, a significant reduction in the total refrigerant charge could be achieved minimizing the liquid separator volume and employing shorter pipes. An optimization of these components and parameters should be performed for the final dimensioning of an actual prototype of the cooling unit.

The dynamic control of the refrigeration system operation is

included in the numerical model. The gas cooler pressure is enforced by a Proportional-Integral (PI) controller as a function of the ambient temperature, to set it to the optimal heat rejection pressure as defined by Liao et al. (2000). In simple back-pressure cycles, the gas cooler pressure is controlled by a PI controller acting on the opening ratio of the HPVs; in ejector cycles, instead, it is controlled by a PI controller acting on the compressor speed, while the HPVs are fully closed. In ejector cycles, the opening ratio of the EVs in front of the evaporators is controlled in order to enforce the evaporation pressure, and consequently the pressure lift, leading to the optimal operation point of the ejectors resulting from the performance maps presented in Fig. 3. In dynamic pulldown operation, the system is controlled to firstly perform MT operation to reach the temperature setpoint in the MT compartment of the insulated box. Once the MT setpoint is reached, the system control turns off the compressor and the unit is switched to LT operation, until the temperature setpoint in the LT compartment is achieved.

The inertia and the limited response time of all the system actuators (compressor, fans, valves) have been synthetically described by including first order delays between the control signals and the actual responses of the components.

The complete description of the dynamic numerical modelling approach and the entire formulation of the differential equations used to describe the dynamic behaviour of the refrigeration system can be found in previous papers published by the same authors: Artuso et al. (2020) and Fabris et al. (2021).

4. Numerical results

The cooling unit is firstly characterized in steady-state conditions, to critically discuss the dimensioning and the performance of the system. The results are assessed through evaluation of the steady-state response of the system to different set-points (compressor speed in case of back-pressure cycle operation and ejector pressure lift in case of ejector cycle operation).

After that, the pull-down of the system from environmental temperature conditions towards the set-point internal temperatures is discussed as an example of the dynamic response of the system.

4.1. Steady-state operation: back-pressure cycle

The steady-state performance of the system is firstly evaluated in its simplest configuration, i.e. back-pressure cycle operation.

In MT operation, the cooling unit provides the necessary cooling effect to achieve the temperature set-point of the internal air ($T_i = 0^{\circ}\text{C}$). The steady-state MT cooling power (Q_{MT}), the compressor power draw

(P_{comp}), the system COP (defined in Eq. (1)) and the evaporation temperature (T_{ev}) of the back-pressure cycle are reported in Fig. 4 as functions of the compressor speed, for ambient temperature equal to $T_{amb} = 15^\circ\text{C}$ (Fig. 4(a)) and $T_{amb} = 30^\circ\text{C}$ (Fig. 4(b)).

$$COP = \frac{Q_{MT}}{P_{comp}} \quad (1)$$

For both ambient conditions, the cooling power and the compressor power draw obviously increase with increasing compressor speed. An MT cooling effect ranging from 3.4 kW to 4.6 kW can be provided for $T_{amb} = 15^\circ\text{C}$, while ranging from 2.6 kW to 4.2 kW for $T_{amb} = 30^\circ\text{C}$. The cooling unit COP decreases with increasing compressor speed, ranging from 2.3 to 4.1 for $T_{amb} = 15^\circ\text{C}$, and from 1.6 to 2.2 for $T_{amb} = 30^\circ\text{C}$, as the evaporation temperature decreases for increasing compressor speed, with a value between -3.8°C and -5.0°C for $T_{amb} = 15^\circ\text{C}$ and between -2.9°C and -4.6°C for $T_{amb} = 30^\circ\text{C}$.

In LT operation, the temperature set-point of the internal air is equal to $T_i = -20^\circ\text{C}$. The steady-state performance of the back-pressure cycle in LT operation, including the system COP as defined in Eq. (2), is reported in Fig. 5 as a function of the compressor speed, for ambient temperature equal to $T_{amb} = 15^\circ\text{C}$ (Fig. 5(a)) and $T_{amb} = 30^\circ\text{C}$ (Fig. 5(b)).

$$COP = \frac{Q_{LT}}{P_{comp}} \quad (2)$$

The system performance as a function of the compressor speed follows the same trend discussed in Fig. 4, with an increase of the compressor power draw and LT cooling effect (1.4 kW – 2.6 kW for $T_{amb} = 15^\circ\text{C}$ and 1.0 kW – 2.1 kW for $T_{amb} = 30^\circ\text{C}$) with increasing compressor speed, while the cooling unit COP (1.4 – 1.7 for $T_{amb} = 15^\circ\text{C}$ and 0.9 – 1.0 for $T_{amb} = 30^\circ\text{C}$) and the evaporation temperature (-26.0°C – -30.0°C for $T_{amb} = 15^\circ\text{C}$ and -24.2°C – -27.8°C for $T_{amb} = 30^\circ\text{C}$) decrease with increasing compressor speed.

It is important to point out that, in LT operations at high ambient temperature ($T_{amb} > 30^\circ\text{C}$) the compressor pressure ratio overcomes the maximum allowed value, thus posing a technological limit to the implementation of the back-pressure cycle. The introduction of the LT ejector, providing a pressure lift between evaporation pressure and compressor suction pressure, can help overcoming this issue, as it will be described in the following sections.

4.2. Steady-state operation: ejector cycle

The use of an ejector in the cooling unit schematic has the main objective of recovering part of the expansion work of the refrigerant mass flow rate after heat rejection to the environment to provide a pressure lift of the mass flow rate at the outlet of the evaporator up to the liquid separator pressure level, thus reducing the compression power requirement. Moreover, in LT operations, the ejector allows the use of a single stage compressor even in high ambient temperature conditions, as it will be detailed in the following discussion.

In the ejector cycle, the compressor speed is controlled to feed the ejector with the exact mass flow rate which can be elaborated by its motive nozzle. On the contrary, the set-point parameter is the pressure lift, which is adjusted through the opening of the evaporator expansion valve.

The performance of the cooling unit operating in ejector configuration for ambient temperature equal to $T_{amb} = 30^\circ\text{C}$ is presented in Fig. 6. The motive energy of the refrigerant mass flow rate at $T_{amb} = 15^\circ\text{C}$ is insufficient to allow the ejector operation. Fig. 6(a) refers to the performance in MT cooling effect production, while Fig. 6(b) refers to LT cooling effect production.

For MT operation (Fig. 6(a)), the cooling power is almost unchanged and equal to approximately 3.8 kW regardless of the ejector pressure lift, while the compressor power draw decreases for increasing lift, therefore increasing the maximum system COP, which reaches its maximum value (equal to 2.3) for a pressure lift of 5.5 bar. However, for pressure lifts higher than 5.5 bar, the decrease in the refrigerant mass flow rate inside the evaporator, due to the reduction of the ejector entrainment ratio with increasing lift, leads to a reduction of the heat transfer coefficient and increase of superheating and to a consequent sudden reduction of the evaporation temperature. Therefore, the separator pressure, corresponding to the compressor suction pressure, starts decreasing, progressively reducing the system COP. The same behaviour can be observed in LT operation (Fig. 6(b)), with an even more significant drop of the system performance for high pressure lifts. In LT operation, a cooling effect production of approximately 1.1 kW and a maximum unit COP of 1.4, corresponding to a pressure lift equal to 5.5 bar, are obtained.

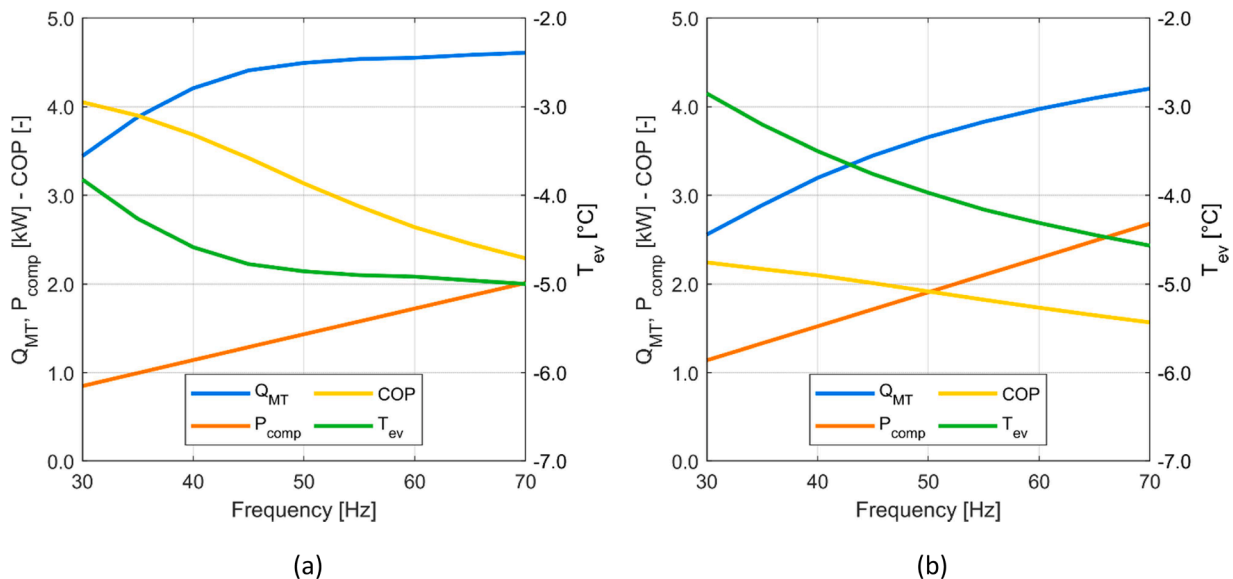


Fig. 4. Performance of the cooling unit in MT operation with back-pressure cycle: (a) with ambient temperature equal to $T_{amb} = 15^\circ\text{C}$; (b) with ambient temperature equal to $T_{amb} = 30^\circ\text{C}$.

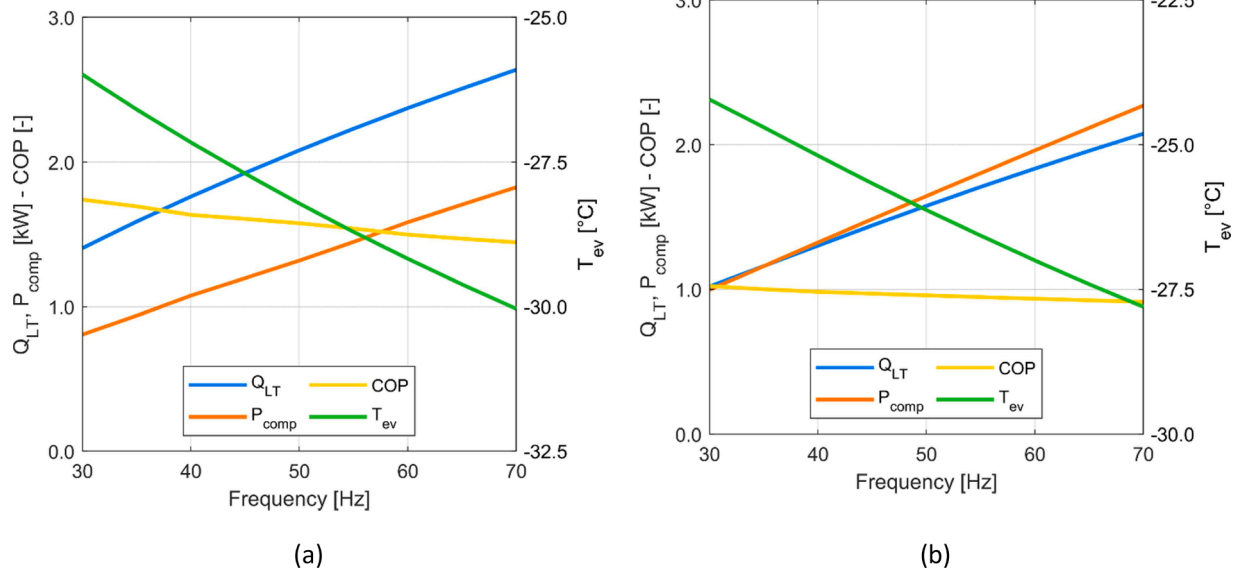


Fig. 5. Performance of the cooling unit in LT operation with back-pressure cycle: (a) with ambient temperature equal to $T_{amb} = 15^\circ\text{C}$; (b) with ambient temperature equal to $T_{amb} = 30^\circ\text{C}$.

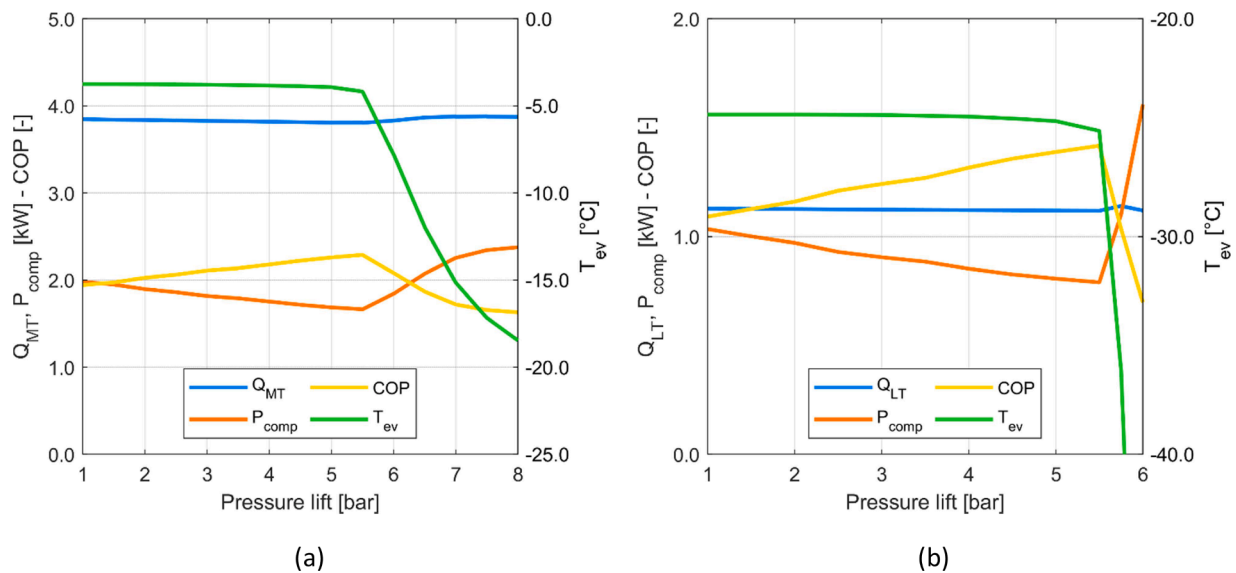


Fig. 6. Performance of the cooling unit with ejector cycle, with ambient temperature equal to $T_{amb} = 30^\circ\text{C}$: (a) MT operation; (b) LT operation.

4.3. Steady-state operation: cycle comparison

To determine the benefits of operating in back-pressure or ejector configuration, the performance of the cooling unit, evaluated in the set of operating conditions considered in Section 4.1 (Figs 4b, 5b, 6a and 6b), is compared in terms of its objective functions, i.e. the cooling effect production and the unit COP, between the two possible configurations and for both MT and LT operation. The results at ambient temperature equal to $T_{amb} = 30^\circ\text{C}$ are presented in Fig. 7.

The system maximum COP is achieved with the cooling unit operating in ejector cycle, for both MT and LT operation. In particular, the COP improvement linked to ejector cycle operation compared to simple back-pressure cycle operation is presented in detail in Table 1 and in Table 2 for MT and LT operation, respectively, along with the corresponding operation parameters, such as cooling power, compressor power draw, and evaporation temperature. To ensure a fair comparison in terms of COP, operating conditions characterized by the same cooling

power, corresponding to the one obtained in the ejector cycle optimal operating point, are compared.

The performance at the operating conditions characterized by the highest cycle COP is considered for the ejector configurations, corresponding to a pressure lift equal to 5.5 bar in both MT and LT operation, in accordance with the results presented in Fig. 6. To approximately match these specific cooling effect productions, in the back-pressure cycle configurations the compressor speed needs to be controlled to 55 Hz in MT operation and to 35 Hz in LT operation. For the considered operating conditions, corresponding to a specific cooling effect production, the ejector cycle presents a COP increase, compared to the back-pressure cycle, equal to 25.8% for MT operation and equal to 42.0% for LT operation.

Nevertheless, as clearly depicted in Fig. 7, it must be pointed out that the back-pressure cycle allows a significantly higher flexibility in the range of both MT and LT cooling power production compared to the ejector cycle. The maximum and the minimum values of the cooling

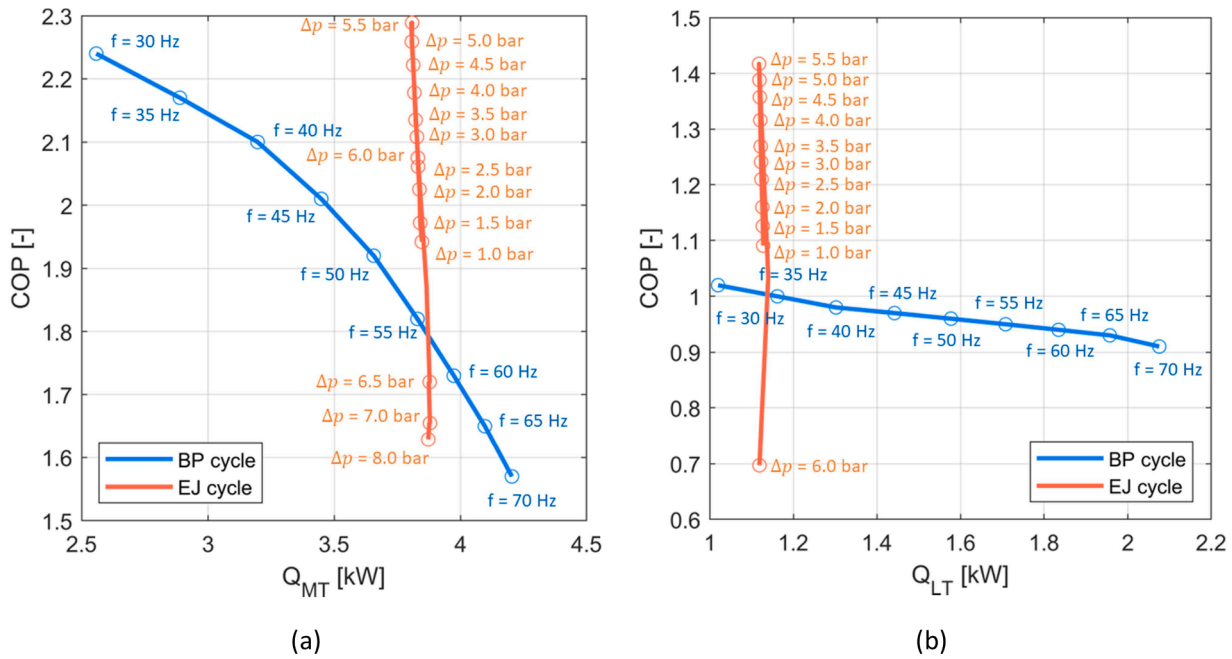


Fig. 7. Performance of the cooling unit terms of cooling effect production and unit COP, with ambient temperature equal to $T_{amb} = 30^{\circ}\text{C}$: (a) MT operation; (b) LT operation.

Table 1

Performance comparison between back-pressure cycle and ejector cycle in MT operation, with ambient temperature equal to $T_{amb} = 30^{\circ}\text{C}$ and equal MT cooling effect production.

	Q_{MT} [kW]	P_{comp} [kW]	COP [-]	T_{ev} [$^{\circ}\text{C}$]	Operating conditions
Back-pressure cycle	3.81	2.09	1.82	-4.18	Compressor frequency = 55 Hz
Ejector cycle	3.81	1.66	2.29	-4.02	MT ejector pressure lift = 5.5 bar

Table 2

Performance comparison between back-pressure cycle and ejector cycle in LT operation, with ambient temperature equal to $T_{amb} = 30^{\circ}\text{C}$ and equal LT cooling effect production.

	Q_{LT} [kW]	P_{comp} [kW]	COP [-]	T_{ev} [$^{\circ}\text{C}$]	Operating conditions
Back-pressure cycle	1.16	1.16	1.00	-24.70	Compressor frequency = 35 Hz
Ejector cycle	1.12	0.79	1.42	-25.15	LT ejector pressure lift = 5.5 bar

power which can be delivered by the cooling unit in back-pressure and ejector configurations are reported in Table 3 and Table 4 for MT and LT operation, respectively.

The back-pressure cycle allows delivering a cooling power down to -32.8% and up to +8.3% in MT operation and a cooling power down to -8.9% and up to +82.5% in LT operation compared to the corresponding

Table 3

Minimum and maximum achievable cooling effect in back-pressure and ejector configurations in MT operation, with ambient temperature equal to $T_{amb} = 30^{\circ}\text{C}$.

	$Q_{MT, min}$ [kW]	$Q_{MT, max}$ [kW]
Back-pressure cycle	2.56	4.20
Ejector cycle	3.81	3.88

Table 4

Minimum and maximum achievable cooling effect in back-pressure and ejector configurations in LT operation, with ambient temperature equal to $T_{amb} = 30^{\circ}\text{C}$.

	$Q_{LT, min}$ [kW]	$Q_{LT, max}$ [kW]
Back-pressure cycle	1.02	2.08
Ejector cycle	1.12	1.14

MT and LT ejector cycle, thus extending significantly the range of achievable cooling effect production of the refrigeration unit, which can be useful in case of high cooling power requirement (i.e., during a pull-down after the opening of the doors of the insulated box) or during part-load operation.

In addition to the above-mentioned considerations, mostly related to performance optimization, functional issues should also be considered. In fact, as it was described in Section 4.1, in ejector configuration, the pressure lift provided by the ejector can help extending the range of environmental conditions in which a single stage compressor can be applied. The evaporation pressures, as well as the compressor suction, discharge and maximum discharge pressures for the operating conditions considered in Table 2 are reported in Table 5.

In case of LT back-pressure cycle operation, the evaporation pressure and the compressor suction pressure coincide, and according to the compressor operability limits, the maximum discharge pressure is equal to 95 bar. Therefore, the LT back-pressure cycle can operate with this evaporation pressure up to a maximum ambient temperature of 34°C . The increase of the compressor suction pressure provided by the ejector lift contribution, while maintaining approximately the same evaporation pressure, allows to extend the operability of the compressor towards

Table 5

Pressure and pressure ratio comparison between back-pressure cycle and ejector cycle in LT operation.

	P_{ev} [bar]	$P_{suction}$ [bar]	P_{HP} [bar]	r_p [-]	$P_{HP, max}$ [bar]
Back-pressure cycle	17.0	17.0	83.0	4.9	95.0
Ejector cycle	16.7	22.2	83.0	3.7	115.0

a discharge pressure up to 115 bar. This is crucial to guarantee the refrigeration system functionality at optimal high-pressure at ambient temperature up to 40°C. While for stationary applications in temperate or continental climate areas such high temperatures can be considered extreme cases, for the given application (on road operation, with possible complete absence of shading) it is critical to consider such conditions.

4.4. Dynamic operation: system pull-down

After the assessment of the steady-state performance of the cooling unit, the dynamic behavior of the system is evaluated through the simulation of a system startup and consequent pull-down from thermal equilibrium with the external environment ($T_{amb} = 30^{\circ}\text{C}$) to the MT and LT temperature set-points. Since the data required for the dynamic characterization of a specific insulated body are not available at this point, the only thermal capacities considered for the following assessment of the system dynamic response are the air volumes inside the MT and LT compartments (approximately 24 m³ and 1 m³, respectively) and the mass of the evaporators (including fans and structural supports). The thermal capacities initialization is done assuming thermal equilibrium with the environment.

The pull-down from thermal equilibrium with the environment at $T_{amb} = 30^{\circ}\text{C}$, performed in ejector configuration, is highlighted in Fig. 8. At the cooling unit startup, the system operates at MT conditions, to reach the set-point temperature $T_{i, MT} = 0^{\circ}\text{C}$ inside the MT compartment. After reaching the MT set-point, the cooling unit is turned off and the system switches to LT cooling effect production, to reach the set-point temperature $T_{i, LT} = -20^{\circ}\text{C}$ inside the LT compartment.

Fig. 8(a) reports the saturation temperature in the liquid separator, in the MT evaporator and in the LT evaporator. Dashed lines are used to highlight the portion of the system which is not operating in each of the sections of the pull-down. The MT pull-down (air inside the MT compartment from 30°C to 0°C) takes around 23 minutes, while the LT pull-down after the configuration switch (air inside the LT compartment from 30°C to -20°C) takes around 40 minutes. Excluding the initial minutes after the system is switched on, it can be observed that both the MT ejector and the LT ejector are able to maintain the optimal pressure lift during dynamic operation.

Fig. 8(b) reports the performance parameters of the system during the pull-down. In the first minutes after the first system switch on in MT operation, the system COP is high because the compression ratio is still limited; on the other hand, after the switch to LT operation, the system COP presents high values because of the high heat transfer in the LT evaporator in the first minutes of operation, due to the significant temperature difference between the air inside the LT compartment (still at 30°C at the beginning of the LT operation) and the saturation temperature of the refrigerant in the evaporator coils (which is already at low values, thanks to the MT pull-down previously performed). However, in both MT and LT operation, as the temperature set-points are approached, the cooling unit performance reaches values which are in agreement with the steady-state values evaluated in Section 4.2.

5. Conclusions and future work

In this study, a novel R744 cooling unit schematic for multi-temperature road transport applications is proposed. The cooling unit is designed to provide MT cooling effect at a temperature equal to 0°C for chilled products and LT cooling effect at a temperature equal to -20°C for frozen products. The system can operate following a simple back-pressure cycle or an ejector cycle, with dedicated MT and LT ejectors. A dynamic numerical model of the cooling unit has been developed to assess at first the steady-state performance of the system under different environmental temperature conditions and with both the possible operating configurations, and then to evaluate the dynamic response of the system during a pull-down from equilibrium with the external environment to the MT and LT temperature set-points.

The use of the ejector for LT operations is intended for both performance improvement and for allowing the use of a single stage compressor in LT operations at high ambient temperature: LT back-pressure configuration is not technically feasible for ambient temperatures above 34°C due to excessive pressure ratio in the compressor, while LT operation can be achieved for ambient temperatures up to 40°C thanks to the pressure lift provided by the ejector.

At ambient temperature equal to 30°C and for a specific cooling effect production (3.8 kW in MT operation, 1.1 kW in LT operation), the ejector cycle leads to a COP increase, compared to the back-pressure cycle, equal to 25.8% for MT operation and equal to 42.0% for LT

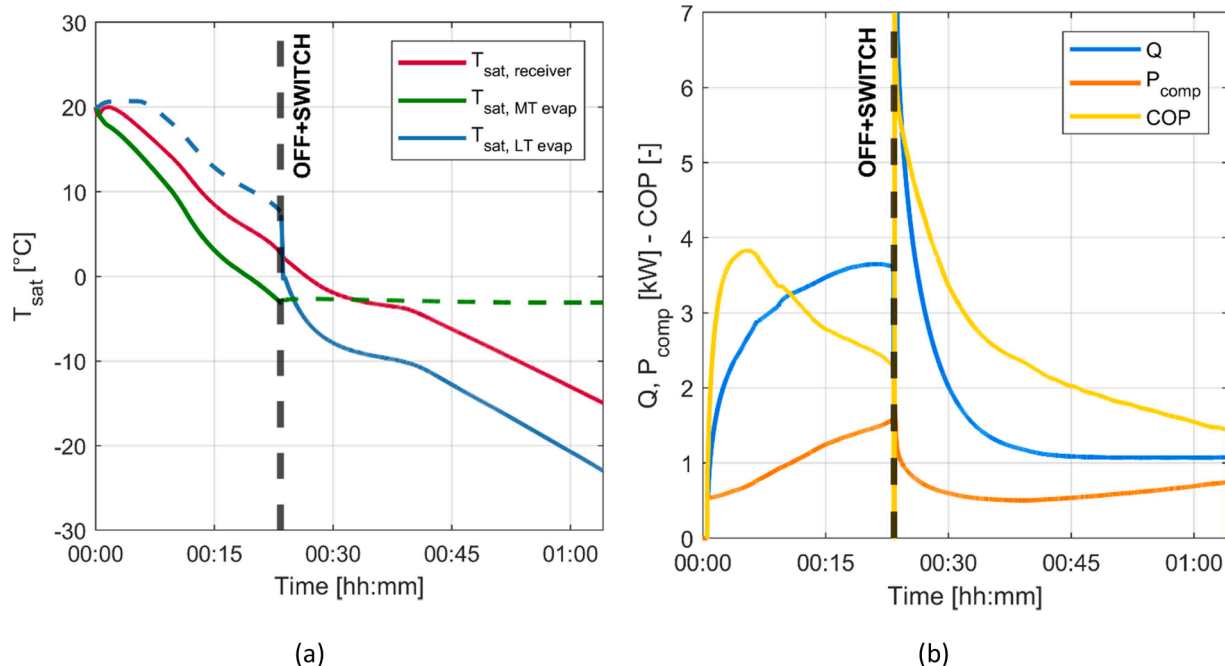


Fig. 8. System pull-down from thermal equilibrium with environment at $T_{amb} = 30^{\circ}\text{C}$: (a) saturation temperatures; (b) cooling unit performance.

operation. Nevertheless, the back-pressure cycle allows a significantly higher flexibility in the range of cooling power production compared to the ejector cycle, for both MT operation (-32.8% - +8.2%) and LT operation (-8.9% - +82.5%), which can be useful during pull-down or part-load operation, as off-design conditions might occur frequently in transport refrigeration applications.

After a switch on from thermal equilibrium with the environment at 30°C, the system, operating in ejector configuration, takes around 23 minutes to reach the MT set-point temperature (0°C) inside the MT compartment and around 40 minutes to reach the LT set-point temperature (-20°C) inside the LT compartment of the refrigerated vehicle, assessing the performance of the ejector cycle also during a pull-down.

Future work will involve a test campaign on MT and LT ejectors prototypes, to experimentally assess the performance of the MT and LT ejectors, specifically designed for the presented application, under different operating conditions. In addition, the numerical model described in this work will be used for the final sizing of the components and for the dynamic evaluation of the system behaviour during standard delivery missions, with the objective of future realization of a complete prototype of the refrigeration unit to be tested in the laboratory and on the field.

Declaration of Competing Interest

The authors declare the following financial interests/personal relationships which may be considered as potential competing interests:

Silvia Minetto reports financial support was provided by European Union.

Acknowledgements

This manuscript is an extended version of the conference paper “Dynamic numerical modelling of a single stage dual temperature R744 ejector-supported refrigeration unit for last mile delivery” by the same authors, presented at the 26th IIR-International Congress of Refrigeration | August 21-25, 2023 | Paris, France. Part of the activity described in this manuscript has been performed within the project ENOUGH. ENOUGH has received funding from the European Union’s Horizon 2020 research and innovation program under grant agreement No 101036588.

References

- Ansys (2023). Available online: <https://www.ansys.com/>.
- Artuso, P., Marinetti, S., Minetto, S., Col, D., Del, Rossetti, A., 2020. Modelling the performance of a new cooling unit for refrigerated transport using carbon dioxide as the refrigerant. *International Journal of Refrigeration* 115, 158–171. <https://doi.org/10.1016/j.ijrefrig.2020.02.032>.
- Azzolin, M., Cattelan, G., Dugaria, S., Minetto, S., Calabrese, L., Del Col, D., 2021. Integrated CO₂ systems for supermarkets: Field measurements and assessment for alternative solutions in hot climate. *Applied Thermal Engineering* 187, 116560. <https://doi.org/10.1016/j.applthermaleng.2021.116560>.
- Bai, T., Yan, G., Yu, J., 2017. Performance evolution on a dual-temperature CO₂ transcritical refrigeration cycle with two cascade ejectors. *Applied Thermal Engineering* 120, 26–35. <https://doi.org/10.1016/j.applthermaleng.2017.03.091>.
- Banasiak, K., Pardiñas, Á., Kriezi, E., 2019. Modelling and development of high-pressure-lift ejector for low temperature evaporators in R744 refrigeration systems for supermarkets. *Proceedings of the 25th IIR International Congress of Refrigeration*, pp. 24–30. [10.18462/iir.icr.2019.0307](https://doi.org/10.18462/iir.icr.2019.0307). Montreal, Canada.
- Bodys, J., Palacz, M., Haida, M., Smolka, J., Nowak, A.J., Banasiak, K., Hafner, A., 2017. Full-scale multi-ejector module for a carbon dioxide supermarket refrigeration system: Numerical study of performance evaluation. *Energy Conversion and Management* 138, 312–326. <https://doi.org/10.1016/j.enconman.2017.02.007>.
- Cavalier, G., Valet, O., Hardy, M., Bourez, D., Fertel, C., 2023. Study of European F-Gas Regulation impact on refrigerated transport equipment. 26th International Congress of Refrigeration, Paris, France. <https://doi.org/10.18462/iir.icr.2023.0922>. August 21–25, 2023.
- Churchill, S.W., 1977. Friction-factor equation spans all fluid flow regimes. *Chemical Engineering Journal* 84, 91–92.
- Dorin (2022). CD Series. Semi-hermetic motor compressors. Transcritical CO₂ application - 50/60 Hz. Available online: https://www.dorin.com/documents/Dorinload/18/LTZ016_CD_02.22.pdf <https://enough-emissions.eu/>. Access 08.09.2023.
- Elbel, S., Hrnjak, P., 2008. Experimental validation of a prototype ejector designed to reduce throttling losses encountered in transcritical R744 system operation. *International Journal of Refrigeration* 31, 411–422. <https://doi.org/10.1016/j.ijrefrig.2007.07.013>.
- European Commission (2014). Regulation (EU) No 517/2014 of the European Parliament and of the Council of 16th April 2014 on fluorinated greenhouse gases and repealing Regulation (EC) No 842/2006.
- Fabris, F., Artuso, P., Marinetti, S., Minetto, S., Rossetti, A., 2021. Dynamic modelling of a CO₂ transport refrigeration unit with multiple configurations. *Applied Thermal Engineering* 189 (February), 116749. <https://doi.org/10.1016/j.applthermaleng.2021.116749>.
- Fabris, F., Fabrizio, M., Marinetti, S., Rossetti, A., Minetto, S., 2023a. Evaluation of the carbon footprint of HFC and natural refrigerant transport refrigeration units from a life-cycle perspective. *International Journal of Refrigeration*. <https://doi.org/10.1016/j.ijrefrig.2023.12.018>.
- Fabris, F., Pardiñas, Á., Marinetti, S., Rossetti, A., Hafner, A., Minetto, S., 2023b. A novel R744 multi-temperature cycle for refrigerated transport applications with low-temperature ejector: experimental ejector characterization and thermodynamic cycle assessment. *International Journal of Refrigeration*. <https://doi.org/10.1016/j.ijrefrig.2023.05.003>.
- Fertel, C., Cavalier, G., Engelmann, P., 2023. Situation and perspectives of evolution of the French refrigerated transport fleet. 26th International Congress of Refrigeration, Paris, France. <https://doi.org/10.18462/iir.icr.2023.0919>. August 21–25, 2023.
- Frank, M., Ostermeier, M., Holzapfel, A., Hübner, A., Kuhn, H., 2021. Optimizing routing and delivery patterns with multi-compartment vehicles. *European Journal of Operational Research* 293 (2), 495–510. <https://doi.org/10.1016/j.ejor.2020.12.033>.
- Friedel, L., 1979. Improved friction pressure drop correlations for horizontal and vertical two-phase flow. *3R Int* 18 (7), 485–491.
- Gnielinski, V., 1976. New equations for heat and mass transfer in turbulent pipe and channel flow. *International Chemical Engineering* 16, 359–368.
- Gullo, P., Hafner, A., Banasiak, K., 2018. Transcritical R744 refrigeration systems for supermarket applications: Current status and future perspectives. *International Journal of Refrigeration* 93, 269–310. <https://doi.org/10.1016/j.ijrefrig.2018.07.001>.
- Gullo, P., Hafner, A., Banasiak, K., Minetto, S., Kriezi, E.E., 2019. Multi-Ejector Concept: A Comprehensive Review on its Latest Technological Developments. *Energies* 12, 406. <https://doi.org/10.3390/en12030406>, 2019.
- Haida, M., Smolka, J., Hafner, A., Ostrowski, Z., Palacz, M., Madsen, K.B., Försterling, S., Nowak, A.J., Banasiak, K., 2018. Performance mapping of the R744 ejectors for refrigeration and air conditioning supermarket application: A hybrid reduced-order model. *Energy* 153, 933–948. <https://doi.org/10.1016/j.energy.2018.04.088>.
- Heßler, K., 2021. Exact algorithms for the multi-compartment vehicle routing problem with flexible compartment sizes. *European Journal of Operational Research* 294 (1), 188–205. <https://doi.org/10.1016/j.ejor.2021.01.037>.
- Karampour, M., Sawalha, S., 2018. State-of-the-art integrated CO₂ refrigeration system for supermarkets: A comparative analysis. *International Journal of Refrigeration* 86, 239–257. <https://doi.org/10.1016/j.ijrefrig.2017.11.006>.
- Liao, S.M., Zhao, T.S., Jakobsen, A., 2000. A correlation of optimal heat rejection pressures in transcritical carbon dioxide cycles. *Applied Thermal Engineering* 20 (9), 831–841. [https://doi.org/10.1016/S1359-4311\(99\)00070-8](https://doi.org/10.1016/S1359-4311(99)00070-8).
- McQuiston, F., 1978. Correlation of heat, mass and momentum transport coefficients for plate-fin-tube heat transfer surfaces with staggered tubes. *ASHRAE Transaction* 84 (1), 294–309.
- Minetto, S., Fabris, F., Marinetti, S., Rossetti, A., 2023. A review on present and forthcoming opportunities with natural working fluids in transport refrigeration. *International Journal of Refrigeration*. <https://doi.org/10.1016/j.ijrefrig.2023.04.015>.
- Ostermeier, M., Henke, T., Hübner, A., Wäscher, G., 2021. Multi-compartment vehicle routing problems: State-of-the-art, modeling framework and future directions. *European Journal of Operational Research* 292 (3), 799–817. <https://doi.org/10.1016/j.ejor.2020.11.009>.
- Palacz, M., Smolka, J., Fic, A., Bulinski, Z., Nowak, A.J., Banasiak, K., Hafner, A., 2015. Application range of the HEM approach for CO₂ expansion inside two-phase ejectors for supermarket refrigeration systems. *International Journal of Refrigeration* 59, 251–258. <https://doi.org/10.1016/j.ijrefrig.2015.07.006>.
- Pardiñas, Á., Hafner, A., Banasiak, K., 2018. Novel integrated CO₂ vapour compression racks for supermarkets. Thermodynamic analysis of possible system configurations and influence of operational conditions. *Applied Thermal Engineering* 131, 1008–1025. <https://doi.org/10.1016/j.applthermaleng.2017.12.015>.
- Peris Pérez, B., Expósito Carrillo, J.A., Sánchez de La Flor, F.J., Salmerón Lissén, J.M., Morillo Navarro, A., 2021. Thermoeconomic analysis of CO₂ Ejector-Expansion Refrigeration Cycle (EERC) for low-temperature refrigeration in warm climates. *Applied Thermal Engineering* 188, 116613. <https://doi.org/10.1016/j.applthermaleng.2021.116613>.
- Shah, M., 1979. A general correlation for heat transfer during film condensation inside pipes. *International Journal of Heat and Mass Transfer* 22, 547–556.
- Smolka, J., Bulinski, Z., Fic, A., Nowak, A.J., Banasiak, K., Hafner, A., 2013. A computational model of transcritical R744 ejector based on a homogeneous real fluid approach. *Applied mathematical modelling* 37 (3), 1208–1224. <https://doi.org/10.1016/j.apm.2012.03.044>.

Steiner, D., Taborek, J., 1992. Flow boiling heat transfer in vertical tubes correlated by an asymptotic model. *Heat Transfer Engineering* 13, 322–329.

United Nations (2022). Agreement on the International Carriage of Perishable Foodstuffs and on the Special Equipment to be Used for Such Carriage (ATP). UNECE Transport Division, Geneva, Switzerland. <https://unece.org/text-and-status-agreement>.

Yang, D., Zhu, J., Wang, N., Xie, J., 2022. Experimental study on the performance of trans-critical CO₂ two-stage compression refrigeration system with and without an ejector at low temperatures. *International Journal of Refrigeration*. <https://doi.org/10.1016/j.ijrefrig.2022.11.019>.